Evidence of porcine and human endothelium activation by cancer-associated carbohydrates expressed on glycoproteins and tumour cells

Olga V. Glinskii[1], James R. Turk[2], Kenneth J. Pienta[3], Virginia H. Huxley[1,2] and Vladislav V. Glinsky[4]

Departments of [1]Medical Pharmacology and Physiology, [2]Biomedical Sciences and [3]Biochemistry, University of Missouri, Columbia, MO 65212, USA
[4]Departments of Internal Medicine and Urology, University of Michigan, Ann Arbor, MI 48109, USA

It is well established that after metastatic cancer cells escape the primary tumour and enter the circulation, their interactions with microvascular endothelium of a target organ constitute an essential rate-limiting step in haematogenous cancer metastasis. However, the physiological and biochemical processes supporting neoplastic cell arrest and retention in the microcirculation are still poorly understood. In this study, we present experimental evidence that microvascular endothelium of metastasis-prone tissues undergoes activation in response to desialylated cancer-associated carbohydrate structures such as Thomsen–Friedenreich (TF) antigen (Galβ1–3GalNAc) expressed on circulating glycoproteins and neoplastic cells. The metastasis-associated endothelium activation, manifested by marked increase in endothelial cell surface galectin-3 expression, causes gradual decrease in cancer cell velocities (from $72 \times 10^2 \pm 33 \times 10^2$ μm s^{-1} to $7.6 \times 10^2 \pm 1.9 \times 10^2$ μm s^{-1}, mean $\pm$ S.D.) accompanied by a corresponding increase in the percentage of rolling cells (from 3.3% $\pm$ 1.2% to 24.3% $\pm$ 3.6%, mean $\pm$ S.D.), and results in human breast and prostate carcinoma cell arrest and retention in the microvasculature. This process, which could be of high importance in haematogenous cancer metastasis, was inhibited efficiently by an anti-TF antigen function-blocking antibody. Carbohydrate-mediated endothelial activation could be a process of physiological significance as it probably occurs in the interactions between a variety of circulating constituents and the vessel wall.

(Resubmitted 9 September 2003; accepted after revision 13 October 2003; first published online 17 October 2003)
Corresponding author V. Glinsky: Department of Biochemistry, University of Missouri, M743 Medical Sciences Bldg, Columbia, MO 65212, USA. Email: glinskiivl@missouri.edu

Metastatic tumour cell adhesion to microvascular endothelium of a target organ represents an essential early step in haematogenous cancer metastasis (Orr & Wang, 2001). The molecular and cellular mechanisms underpinning this process remain poorly understood. For example, in inflammation, leucocyte–endothelium adhesion requires endothelial activation by inflammatory cytokines such as tumour necrosis factor α (TNFα) or interleukin-1β (IL-1β), resulting in a cell surface mobilization of endothelial selectins (reviewed in McEver, 1997), and a coordinated set of highly orchestrated selectin interactions with their cognate carbohydrate ligands, mostly Lewis(x), sialyl-Lewis(x) and sialyl-Lewis(a) core 2 oligosaccharides (Butcher, 1991; Lawrence & Springer, 1991; McEver, 1997), mediating leucocyte rolling and adhesion (Lawrence & Springer, 1991; McEver, 1997). Perhaps with the exception of colon carcinoma (Krause & Turner, 1999), such an activation scheme fails to enhance neoplastic cell adhesion to the endothelium (Cooper *et al.* 2002). Moreover, in a related study, Satoh *et al.* (1998) demonstrated that multiple prostate carcinoma cell lines, expressing sialyl-Lewis(x), the carbohydrate epitope recognized by endothelial selectins supporting leucocyte rolling, lack selectin-dependent adhesion.

These observations suggest that leucocyte and metastatic tumour cell adhesion to microvascular endothelium are driven by different molecular mechanisms. Indeed, recent results demonstrate that breast and prostate cancer cell adhesion to the microvascular endothelium of metastasis-prone tissues is mediated largely by interactions between cancer-associated TF glycoantigen (Galβ1–3GalNAc) presented on neoplastic cells and endothelium-expressed β-galactoside binding lectin galectin-3 (Lehr & Pienta,

V.H.H. and V.V.G. share senior authorship.

DOI: 10.1113/jphysiol.2004.054783

1998; Glinsky *et al.* 2000, 2001; Nangia-Makker *et al.* 2002; Khaldoyanidi *et al.* 2003). However, similarly to selectins, galectin-3 is often localized intracellularly (Ellerhorst *et al.* 1999; Glinsky *et al.* 2001). To participate in cell-to-cell adhesive interactions, this carbohydrate-binding protein must be translocated to the endothelial cell surface. Recently, based on the ability of asialofetuin (a glycoprotein expressing multiple TF antigen epitopes) and TF antigen–human serum albumin conjugate (TF–HSA) to increase galectin-3 cell surface expression on cultured endothelial cells (Glinsky *et al.* 2001), we suggested that desialylated cancer-associated carbohydrate structures can induce such translocation, thereby modifying endothelial cell adhesive properties and priming them for binding metastatic cancer cells (Glinsky *et al.* 2001).

In this report, we present *in vitro* and *ex vivo* experimental evidence of microvascular endothelium activation manifested by a marked increase in galectin-3 cell surface expression promoting metastatic breast and prostate carcinoma cell adhesion to the endothelia of intact well-differentiated microvessels. In contrast to leucocyte adhesion, this activation occurs in a non-cytokine-mediated manner and is induced by cancer-associated carbohydrate structures (TF antigen disaccharide) expressed on metastatic tumour cells (direct activation) or circulating glycoproteins (indirect activation), which could often be found in serum of patients with adenocarcinomas of different origin (Bresalier *et al.* 1996; Duffy, 1999). Given the efficient inhibition of this process by anti-TF antigen monoclonal antibody, such activation could be an important target for developing new approaches to preventing and controlling haematogenous breast and prostate cancer metastasis.

Methods

Antibodies, chemicals, and reagents

The TIB-166 hybridoma, producing rat anti-galectin-3 monoclonal antibody (mAb) was obtained from ATCC (Manassas, VA, USA). The JAA-F11 hybridoma producing anti-TF antigen mAb (Rittenhouse-Diakun *et al.* 1998) was from Dr K. Rittenhouse-Olson (State University of New York, Buffalo, NY, USA). All other chemicals and reagents, unless otherwise specified, were from Sigma (St Louis, MO, USA).

Cell lines and cultures

The highly metastatic MDA-MB-435 and non-metastatic MDA-MB-468 human breast carcinoma cell lines were provided by Dr J. E. Price (M.D. Anderson Cancer Center, Houston, TX, USA). The DU-145 metastatic human prostate carcinoma cells were from ATCC. The RPMI-1640 medium supplemented with L-glutamine, 10% fetal bovine serum (FBS), sodium pyruvate and non-essential amino acids was used for tumour cell lines. For adhesion experiments, cancer cells were prelabelled for 5 min with a 3 μg/ml solution of acridine orange in RPMI-1640 medium, rinsed three times with serum free RPMI-1640 medium, dissociated from plastic using a non-enzymatic cell dissociation reagent (Sigma), and pipetted to produce a single cell suspension.

Owing to its rapidity and simplicity, labelling neoplastic cells with acridine orange represents a valuable method of choice for our experiments, in which freshly prepared single cell suspension is required for each round (i.e. every 30 min). Abbitt *et al.* (2000) reported recently that acridine orange could modify the adhesion behaviour of neutrophils by inducing β2-integrin (CD18) expression. However, our previous studies, involving parallel experiments with acridine orange- and dioctadecyl-tetramethylindocarbocyanine ($DiIC_{18}$)-labelled breast and prostate carcinoma cells (Glinsky *et al.* 2000, 2001), did not reveal any significant effects of acridine orange labelling on malignant cell adhesive behaviour. One possible explanation for this could be that β2-integrin does not play a major role in cancer–endothelial cell adhesion. Blocking CD18 function caused only marginal ($< 20\%$) inhibition of prostate cancer cell adhesion to bone marrow endothelium in a static adhesion assay (Lehr & Pienta, 1998), and failed completely to inhibit breast carcinoma cell adhesion to endothelial cells in flow (Khaldoyanidi *et al.* 2003). Another explanation could be that, as the neoplastic cells are labelled with acridine orange for each round immediately prior to preparation and perfusion of the single cell suspension through the microvasculature for 30 min, the time course is not of sufficient length for acridine orange to alter significantly transcriptional processes, which could lead to appreciable changes in the protein expression levels.

Nevertheless, we performed additional parallel flow chamber experiments to compare rolling responses of non-labelled and acridine orange-labelled MDA-MB-435 cells perfused over a monolayer of HBME-1 human bone marrow endothelial cells. The results of these experiments demonstrated that acridine orange did not modify significantly MDA-MB-435 human breast carcinoma cell rolling on HBME-1 monolayers. Specifically, at the wall shear stress of 2.4 dyn cm^{-2}, the rolling flux of non-labelled and acridine orange-labelled MDA-MB-435 cells differed

by <5 % (27.7% ± 2.6%, mean ± S.D., $n = 358$; and 32.1% ± 9.5%, mean ± S.D., $n = 500$, respectively).

The human bone marrow endothelial cell line HBMEC-60, immortalized using the amphotrophic helper-free retrovirus pLXSN16 E6/E7 (Rood *et al.* 2000), was provided by Dr C.E. van der Schoot (University of Amsterdam, Amsterdam, The Netherlands). The HBMEC-60 cells were shown to maintain their normal phenotype and adhesive properties, specifically the ability to bind haematopoietic progenitor cells (Rood *et al.* 2000). The development of the HBME-1 human bone marrow endothelial cell line, immortalized using SV40 large T antigen, was as previously described (Lehr & Pienta, 1998). The basal Medium 200 (Cascade Biologics, Portland, OR, USA) supplemented with 20% FBS and low serum growth supplement containing hydrocortisone, human fibroblast growth factor, heparin and human epidermal growth factor was used for culturing HBMEC-60 and HBME-1.

Perfused porcine dura mater model

Porcine dura mater was used in adhesion experiments as described in detail elsewhere (Glinskii *et al.* 2003*a*,*b*). Briefly, dura mater corresponding to one hemisphere was collected from mature male (for prostate cancer experiments, $n = 12$) or female (for breast cancer experiments, $n = 14$) Yucatan miniature swine (Charles River, ME, USA) within 30 min of death. The animals were killed in accordance with the University of Missouri approved animal care protocol. Dura mater was dissected and flattened on to a Sylgard-coated 100 mm dish. A major branch of the median meningeal artery (typically 300–500 μm i.d.) was cannulated, and dura vasculature was perfused at 15 μl min^{-1} first with Krebs physiological salt supplemented with 1.0 mg ml^{-1} porcine serum albumin for 20 min, then with vessel-labelling solution (0.3 μg ml^{-1} acridine orange in RPMI-1640 supplemented with 10% FBS and 1.0 mg ml^{-1} porcine albumin) for an additional 40 min. In selected experiments, asialofetuin or fetuin were added to the vessel labelling solution at 1.0 mg ml^{-1} final concentration. Asialofetuin is a glycoprotein carrying multiple desialylated TF antigen moieties, whereas fetuin differs from asialofetuin only in that the TF antigen moieties are masked covalently with sialic (neuraminic) acid. In function inhibition experiments, undiluted supernatant from JAA-F11 hybridoma, producing function-blocking antibody against TF antigen, was used instead of RPMI-1640. In addition, to determine the contribution of shear forces, in selected experiments after labelling microvessels with acridine orange, dura mater was preperfused at the above rate for 2 h prior to tumour cell injection.

Immediately prior to injection, cancer cells were prelabelled for 5 min with 3 μg ml^{-1} acridine orange solution in RPMI-1640 medium, rinsed three times, dissociated from plastic, pipetted to produce a single cell suspension, filtered through a 20 μm nylon mesh to remove any remaining cell clumps, and adjusted to contain 5×10^4 cells ml^{-1}. A fresh tumour cell suspension in perfusion buffer (RPMI-1640 supplemented with 10% FBS and 1.0 mg ml^{-1} porcine serum albumin) was prepared for each 30 min round and injected into the system using an inline chromatography injector with all-Teflon wetted parts (Rheodyne Model 50200, Rheodyne, CA, USA) equipped with a 500 μl loop. Cancer cell interactions with dura microvasculature were monitored at several predetermined observation points over 80–100 μm i.d. microvessels (minimum of eight observation points per experiment, i.e. two observation points per round) and video recorded at 30 frames per second using a fluorescence video microscopy system based on a Laborlux 8 microscope (Leitz Wetzlar, Germany) equipped with 75 W xenon lamp and a high sensitivity CCD video camera (COHU Inc., San Diego, CA, USA). For subsequent frame-by-frame analysis, the recorded analog video images were digitized using a media converter DVMC-DA2 (Sony, Japan) and Adobe Premier 6 software (Adobe Systems Inc., San Jose, CA, USA).

Data analysis and interpretation

An offline frame-by-frame analysis was used to determine cancer cell velocities within perfused dura mater microvasculature. Based on velocity measurements and adhesion behaviour, we divided circulating malignant cells into the following categories: non-interacting/freely floating cells, interacting/rolling cells, slow rolling cells, and stably adherent cells.

In our previous studies, employing the same experimental conditions (Glinskii *et al.* 2003*a*,*b*), we determined a velocity limit for distinguishing between non-interacting/floating and interacting/rolling cells within 80–100 μm arterioles of 2000 μm s^{-1}. This determination was made based solely on experimental results, as we observed neoplastic cells moving at velocities as high as 1500– 2000 μm s^{-1} engaging momentarily in stable adhesive interactions with microvessel walls (Fig. 1). However, as early as in 1985–1991, in a series of fundamental works on leucocyte–endothelial interactions (Gaehtgens *et al.* 1985; Ley *et al.* 1991; Ley & Gaehtgens, 1991), Ley and Gaehtgens introduced the term

critical velocity (V_{crit}), defining a minimal velocity that a freely flowing cell can assume under given experimental conditions and developed a formula

$$V_{crit} = V_{CL} \times \varepsilon \times (2 - \varepsilon)$$

where V_{CL} is the velocity of a cell floating at the centreline, and e is the ratio of a cell diameter to the vessel diameter. Any cell travelling at a velocity below V_{crit} is likely to be retarded by adhesive interactions with vascular wall and should be designated as rolling (Ley & Gaehtgens, 1991). Using such a criterion allows for unambiguous identification of cells interacting with vessel wall even in the absence of information on their relative radial position (Ley *et al.* 1991).

We have used the formula developed by Ley & Gaehtgens (1991) to calculate V_{crit} for our experimental conditions, i.e. for tumour cells travelling within 80–100 μm arterioles perfused at the physiological rate. For these calculations, we assumed the average tumour cell velocity of 7200 μm s^{-1} at the beginning of the experiment before endothelium activation occurred (see Results and discussion) as V_{CL}, the average tumour cell diameter to be 15 μm and the average vessel diameter to be 90 μm. The resulting calculated V_{crit} value of 2200 μm s^{-1} appears to be in good agreement with our velocity limit of 2000 μm s^{-1} for identifying interacting/rolling cancer cells within 80–100 μm arterioles established experimentally.

To distinguish a subpopulation of cancer cells interacting with endothelium more specifically, we used several additional velocity and adhesion behaviour criteria to identify slowly rolling tumour cells: (1) clearly visible rolling; (2) frequent stoppages, interruptions and changes in velocity; (3) deviations from a straight-line movement in a zigzag manner; and (4) rolling velocity below 600 μm s^{-1}. The last determination was made based on the fact that mean blood velocities and corresponding wall shear rates in arterioles are about double those in post-capillary venules of the same size (Ley & Gaehtgens, 1991). As velocities up to 300 μm s^{-1} were described for leucocytes rolling in post-capillary venules (Ley & Gaehtgens, 1991), we established a 600 μm s^{-1} velocity limit for identifying cancer cells slowly rolling in 80–100 μm arterioles. In this report, we will use the term interacting/rolling cells to refer to the population of neoplastic cells travelling at velocities below V_{crit}, whereas the term rolling will be used to refer to the subset of slowly rolling cells.

In contrast to cancer cells transiently interacting with vessel walls and designated as interacting/rolling (rapidly rolling) and slowly rolling, some neoplastic cells were engaged in more stable adhesive interactions and remained stationary for a prolonged period of time (>1 min). For the purpose of this study, such cells were designated as stably adherent.

Analysis of cell surface galectin-3 expression

The *ex vivo* immunofluorescence analysis of intravascular cell surface galectin-3 expression was performed using TIB-166 anti-galectin-3 antibody. After completion of the cancer cell adhesion experiment or asialofetuin perfusion, dura mater was perfused for 30 min with anti-galectin-3 mAb diluted 1 : 10, followed by a 30 min wash, 30 min perfusion with 10.0 μg ml^{-1} solution of Alexa Fluor 594-labelled goat anti-rat IgG (Molecular Probes, Eugene, OR, USA), and an additional 30 min wash. The *in vitro* analysis of cell surface galectin-3 expression on non-fixed and non-permeabilized cultured HBMEC was performed exactly as previously described (Glinsky *et al.* 2001, 2003).

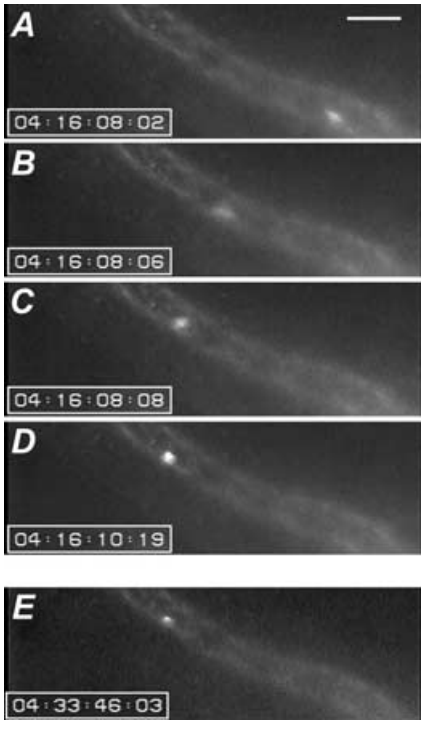

Figure 1. Stable adhesion of a rapidly rolling metastatic cancer cell

The MDA-MB-435 human breast carcinoma cell travelling at 1560 μm s^{-1} (*A*) momentarily stops, (*B*) slightly rolls, (*C*) becomes stably attached to a vascular wall (*D*) and remains stationary until the end of the observation period (*E*). Numbers in boxes show time code generator readings corresponding to each frame in hours, minutes, seconds, and frame numbers (30 frames s^{-1}) presented as hh:mm:ss:ff. The differences in time between images shown are: 0.13 s (between *A* and *B*), 0.67 s (between *B* and *C*), 2.37 s (between *C* and *D*) and over 17 min (between *D* and *E*). Scale bar, 200 μm shown in *A*.

Results

The percentage of cancer cells interacting with microvascular endothelium increases over time as a function of tumour cell–vascular wall collisions

Many important results regarding tumour–endothelial cell interactions have previously been obtained *in vitro* using cultured endothelial cells. However, as endothelial cell properties depend to a large extent on their organ-specific microenvironment (Ruoslahti & Rajotte, 2000) and preserving original microenvironment and temporal dynamics is crucial for obtaining the most accurate and reliable data (Padera *et al.* 2002), we investigated the kinetics of breast and prostate carcinoma cell adhesive interactions with intact well-differentiated microvessels of dura mater, a tissue often targeted by haematogenous cancer metastasis (Rubin *et al.* 2000). In these experiments, we analysed tumour cell velocities and percentage of interacting/rolling cancer cells within dura mater microvasculature perfused at the physiological flow rate (15 μl min^{-1}) with a single cell suspension (5×10^4 cells ml^{-1}) of fluorescently labelled neoplastic cells (metastatic DU-145 prostate carcinoma or MDA-MB-435 breast carcinoma, and non-metastatic MDA-MB-468 breast carcinoma) using experimental techniques developed recently in our laboratory (Glinskii *et al.* 2003*a*,*b*). As we reported, in contrast to leucocyte adhesion, that the vast majority of cancer cell adhesive interactions with microvessels occur in precapillary arterioles (Glinskii *et al.* 2003), we specifically focused on analysing tumour cell adhesion kinetics within an arterial compartment of dura mater microvasculature. Neoplastic cell intravascular adhesive behaviour was monitored and video recorded at several predetermined observation points over 80–100 μm i.d. arterioles, and 500 μl of freshly prepared single cell suspension was injected every 30 min.

Intriguingly, at the beginning of the experiments, perfused metastatic cells moved at high velocities ($72 \times 10^2 \pm 33 \times 10^2$ μm s^{-1}, mean ± s.d.). At this time, only a small fraction (3.3% ± 1.2%, mean ± s.d. of neoplastic cells exhibited slow rolling behaviour and none engaged into stable adhesion either within immediately observed microvessels or within perfused vascular tree. However, as the experiments progressed, we observed a gradual decrease in tumour cell velocity over time with each consecutive injection (Fig. 2*A*). Subsequently, even though the perfusion rate was kept constant, toward the fourth round of experiments (1.5–2 h of perfusion) the average tumour cell velocity decreased almost 10-fold ($7.6 \times 10^2 \pm 1.9 \times 10^2$ μm s^{-1}, mean ± s.d.) compared with the first round and 100% of cells observed travelled at velocities below V_{crit} (Fig. 2*A*).

The observed reduction in tumour cell velocity below V_{crit} probably reflects their displacement toward blood vessel walls and increased adhesive interactions with microvascular endothelium. Indeed, a gradual decrease in metastatic cell velocity was accompanied by a corresponding gradual increase in the percentage of slowly rolling cells (Fig. 2*B*) from 3.3% ± 1.2% to 24.3% ± 3.6% (mean ± s.d.; by the fourth round of the experiment, abundant tumour cell interactions with dura microvasculature were observed along with multiple neoplastic cells stably adhered in precapillary arterioles and capillaries.

We observed consistently this pattern of dynamic changes in metastatic cell–microvascular endothelium adhesion kinetics in both prostate and breast carcinoma

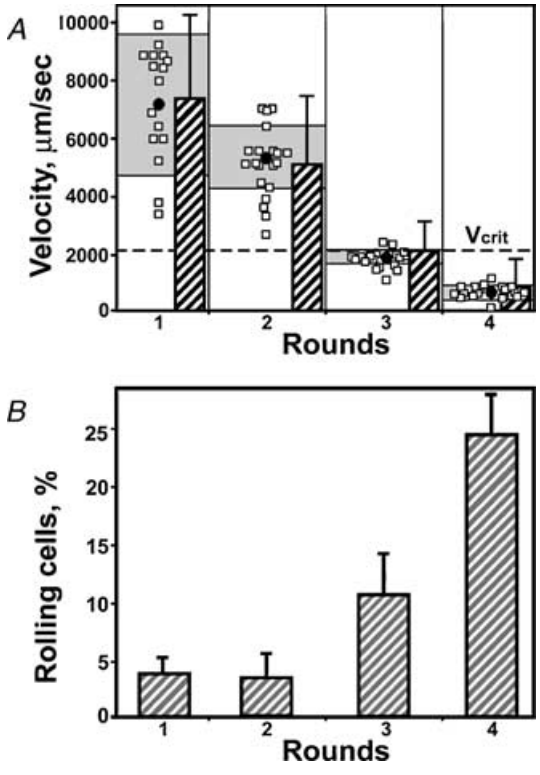

Figure 2. Gradual increase in malignant cell adhesive interactions with microvascular endothelium over time
A, gradual decrease in velocities of DU-145 metastatic prostate carcinoma cells perfused at constant physiological rate (15 μl min^{-1}). Open squares represent individual values; filled circles represent average velocity; shaded area, ± average deviation; each round corresponds to 30 min of perfusion. Bars show combined results of three independent experiments presented as mean + s.d. *B*, gradual increase in the proportion of rolling tumour cells over the course of an adhesion experiment (mean + s.d.).

cell experiments on 14 dura mater preparations (eight males, six females, respectively). These results imply that adhesive properties of either endothelial or cancer cells (or both) undergo significant modification over the course of an experiment. However, as the single cell suspension of tumour cells was prepared freshly prior to each injection, i.e. every 30 min, the observed changes in kinetics of metastatic cell interactions with perfused microvasculature probably reflect changes in endothelial cell adhesiveness. In other words, upon perfusion with metastatic cancer cells, microvascular endothelium undergoes activation promoting malignant cell rolling and retention in the target organ microvasculature. Furthermore, this metastasis-associated endothelium activation appears to be mediated not by shear force, but rather by tumour cell collisions with vascular walls, as preperfusing microvessels for the same time period (2 h) in the absence of cancer cells did not modify tumour cell–microvascular endothelium adhesion kinetics (data not shown). This, in turn, suggests the existence of one or more factors responsible for such activation presented on malignant cell outer surfaces. Recently, based on the ability of cancer-associated TF glycoantigen expressed on asialofetuin and TF antigen–human serum albumin conjugate to increase galectin-3 cell surface expression on cultured endothelial cells, we suggested that TF antigen expressed on neoplastic cells and circulating tumour-secreted glycoproteins could potentially perform such function (Glinsky *et al.* 2001). We next investigated whether TF antigen is indeed responsible for changes in kinetics of metastatic cell interactions with dura microvessels.

Cancer cells and asialofetuin activate microvascular endothelium in a TF antigen-dependent manner

We have used several independent approaches to address this question. First, we investigated whether non-metastatic MDA-MB-468 breast carcinoma cells, deficient in TF antigen expression (Khaldoyanidi *et al.* 2003), would exhibit similar intravascular adhesion kinetics as highly metastatic DU-145 (Fig. 2*A*) and MDA-MB-435 (Fig. 3*A*) cells. The results of these experiments demonstrated that, in contrast to highly metastatic cells expressing significant TF antigen levels (Glinsky *et al.* 2000, 2001), MDA-MB-468 neither exhibited a decrease in velocity (Fig. 3*A*) nor engaged into adhesive interactions with dura microvessels. Next, we studied the effects of function blocking anti-TF antigen antibody on adhesion kinetics of highly metastatic MDA-MB-435 cells. Perfusing MDA-MB-435 cells in the presence of anti-TF antibody almost completely abolished the gradual decrease in tumour cell velocity (Fig. 3*A*), as well as the subsequent metastatic cell arrest in microvessels (Fig. 3*C* and *D*). Finally, we investigated whether asialofetuin, a glycoprotein carrying multiple TF antigen moieties, would activate microvascular endothelium in a TF antigen-dependent manner. Pre-perfusing dura mater with asialofetuin (1.0 mg ml^{-1} final concentration) resulted in an immediate (first round of perfusion) decrease in tumour cell velocities to below those recorded in the fourth round of the control experiments, which remained at these levels throughout the experiment (Fig. 3*A*). The asialofetuin-mediated decrease in tumour cell velocities was accompanied by a dramatic increase in a fraction of slowly rolling cancer cells (Fig. 3*B*). Importantly, pre-incubation of asialofetuin with anti-TF antigen function-blocking antibody abolished completely asialofetuin effects on metastatic cell velocities (data not shown), proportion of rolling cells (Fig. 3*B*), and metastatic cell arrest and retention in microvessels (Fig. 3*E* and *F*). These outcomes indicate that TF antigen is indeed a structure responsible for metastasis-associated endothelium activation. Of note, fetuin, which is identical to asialofetuin but has TF antigen epitopes masked covalently with sialic acid, did not modify the kinetics of tumour cell interactions with microvascular endothelium (data not shown).

Endothelium activation by tumour cells and asialofetuin is manifested by the increased cell surface galectin-3 expression on microvessels

Previously, we reported that both asialofetuin (Glinsky *et al.* 2001) and TF antigen-expressing tumour cells (Khaldoyanidi *et al.* 2003) cause rapid increase in cell surface expression of β-galactoside-binding lectin galectin-3 on cultured endothelial cells. Subsequently, endothelium-expressed galectin-3 acts as a binding partner for TF antigen on cancer cells (Glinsky *et al.* 2001), and tumour–endothelial cell adhesion is mediated largely by TF antigen–galectin-3 interactions (Glinsky *et al.* 2001, 2003; Khaldoyanidi *et al.* 2003). Therefore, we investigated next whether metastatic cancer cell and asialofetuin effects upon well-differentiated microvessels *ex vivo* modify intravascular galectin-3 levels as well. The results of these experiments demonstrated that metastasis-associated microvascular endothelium activation induced by both malignant cells (Fig. 4*B* and *C*) and asialofetuin (Fig. 4*D*) was manifested by a marked increase in galectin-3 cell surface expression on microvascular endothelium.

However, intriguingly, elevated cell surface galectin-3 expression was detectable only in selected segments of particular microvessels (mostly precapillary arterioles ranging from 50 μm to 100 μm in diameter), suggesting that not all microvessels respond uniformly to TF antigen-mediated stimuli.

This phenomena was of particular note because our previous experiments revealed that the vast majority of neoplastic cell adhesive interactions with microvasculature occur in precapillary arterioles and capillaries (Glinskii *et al.* 2003), and that even within the arterial microcirculatory compartment different segments of the same vessel exhibit differential ability to bind tumour cells. We observed frequently multiple stably adhered tumour cells located within relatively short segments of precapillary arterioles, whereas the rest of the vessel as well

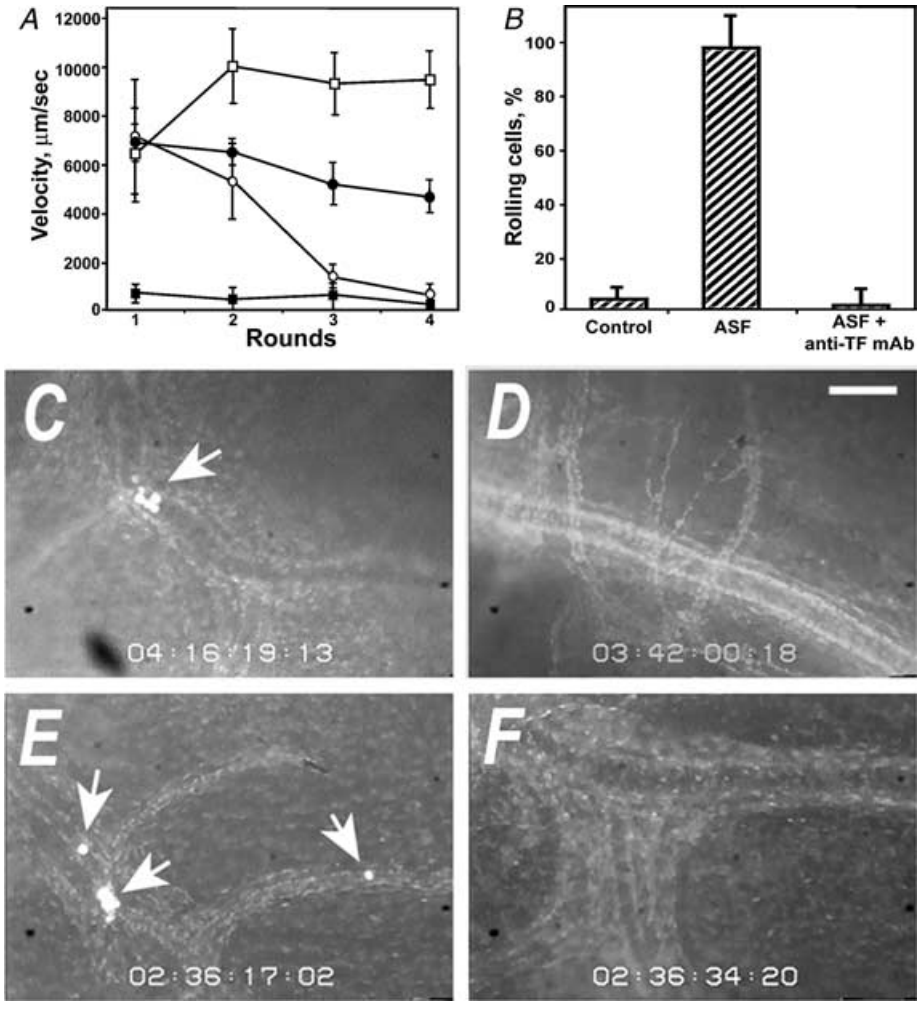

Figure 3. Cancer cells and asialofetuin activate microvascular endothelium in a TF antigen-dependent manner

A, similar to DU-145 prostate carcinoma cells (Fig. 2), highly metastatic MDA-MB-435 breast cancer cells (open circles), expressing elevated TF antigen levels, exhibit a gradual decrease in velocity over the course of the adhesion experiment (each round corresponds to 30 min of perfusion). By contrast, non-metastatic MDA-MB-468 cells (open squares), deficient in TF antigen expression, do not demonstrate such a decrease. Anti-TF antigen mAb abolishes MDA-MB-435 decrease in average velocity (filled circles). Microvascular endothelium stimulation with asialofetuin, a glycoprotein carrying multiple TF antigen moieties (filled squares), results in the immediate drop in MDA-MB-435 cell velocities below the fourth round control values (open circles), accompanied by a dramatic increase in the proportion of rolling cells (*B*), which was inhibited completely by anti-TF antigen mAb. *C*, stable adhesion of MDA-MB-435 breast cancer cells after the fourth round of perfusion inhibited by anti-TF antigen antibody (*D*). *E*, stable adhesion of MDA-MB-435 breast cancer cells to asialofetuin-stimulated microvasculature after the first round of perfusion inhibited by anti-TF antigen antibody (*F*). Scale bar, 200 μm.

as neighbouring microvessels remained free of malignant cells (Fig. 4*E*). This observation suggested the existence of endothelial 'hot spots' within a microcirculation of metastasis-prone organs, which possess an enhanced ability to bind and retain metastatic cells compared with the rest of the microvasculature. We investigated next whether such 'hot spots' harbouring multiple tumour cells correspond to the areas of elevated intravascular galectin-3 expression. The results of these experiments (Fig. 4*F* and *G*) showed that multiple stably adhered breast and prostate carcinoma cells do indeed reside in microvessel segments expressing elevated galectin-3 levels. These results further supported the idea that metastasis-associated endothelium activation mediated by tumour-associated carbohydrate structures and manifested by elevated cell surface galectin-3 expression could be important in metastatic cell arrest in the microcirculation of target organs.

To determine whether cancer-associated carbohydrates (TF antigen) would activate in a similar manner microvascular endothelium derived from other metastasis-prone tissues, we investigated the effects of asialofetuin on the galectin-3 expression on HBMEC *in vitro*. Similar to dura mater microvasculature, HBMEC responded to asialofetuin treatment by a rapid and significant increase in cell surface galectin-3 expression (Fig. 5). The asialofetuin effect on HBMEC was inhibited almost completely by anti-TF antigen mAb, again emphasizing the important role for this carbohydrate structure in metastasis-associated endothelium activation. Of note, in these *in vitro* experiments as well, only selected endothelial cells responded to asialofetuin stimulation, suggesting that even established endothelial cell lines preserve their heterogeneity regarding the ability to respond to carbohydrate stimuli.

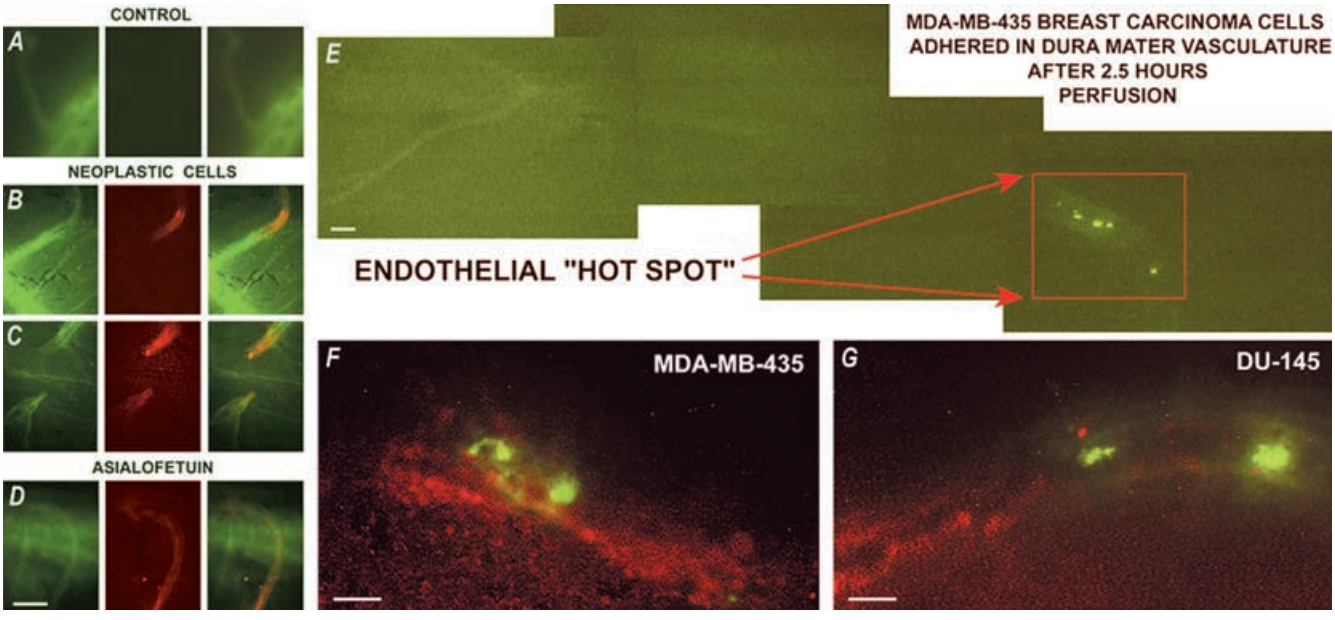

Figure 4. Metastasis-associated endothelium activation manifested by elevated intravascular galectin-3 expression

A–D, the perfusion of dura mater microvasculature with either metastatic breast (*B*) or prostate (*C*) tumour cells or asialofetuin (*D*) mediates elevated cell surface galectin-3 expression in selected segments of precapillary arterioles compared with the control (*A*). Left-hand panels, green fluorescence of dura mater microvessels labelled with acridine orange. Middle panels, red fluorescence associated with cell surface galectin-3. Right-hand panels, superimposed images showing the association of cell surface galectin-3 expression with selected segments of pre capillary arterioles. *E–G*, endothelial 'hot spots' correspond to areas with increased cell surface galectin-3 expression. *E*, endothelial 'hot spot' harbouring multiple metastatic breast carcinoma cells, whereas the rest of the microvasculature is free of tumour cells. *F* and *G*, multiple breast (*F*) and prostate (*G*) carcinoma cells adhered in precapillary arteriole segments with elevated galectin-3 expression (red fluorescence). Scale bar in *A–D* (shown in *D*), 200 μm; *E–G*, 50 μm.

Discussion

According to hydrodynamic studies, Poiseuille flow in blood vessels, characterized by a parabolic profile (Fig. 6), forces larger particles, such as non-interacting leucocytes or cancer cells, to the centre of the stream (Segre & Silberberg, 1962; Lawrence & Springer, 1991). Therefore, at a constant perfusion rate, the observed gradual reduction in tumour cell velocity (V_1–V_2) reflects their displacement (Δ) out from the centre stream toward the blood vessel wall (Fig. 6), whereas both direct tumour cell interactions with vascular wall and the difference in torque (T_1–T_2) acting upon malignant cell edges located distally and proximally to a vascular wall regulate rolling response (Lawrence & Springer, 1991). So increasing the proprotion of cancer cells travelling at velocities below V_{crit}, which are likely to be retarded by adhesive interactions with vascular wall (Ley & Gaehtgens, 1991), reflects the gradual increase in endothelium adhesiveness resulting from metastasis-associated endothelium activation.

As we observe essentially horizontally positioned microvessels, one can argue that sedimentation as a result of gravity could affect tumour cell radial position and cause their margination (Fig. 7*A*), which in turn may lead to

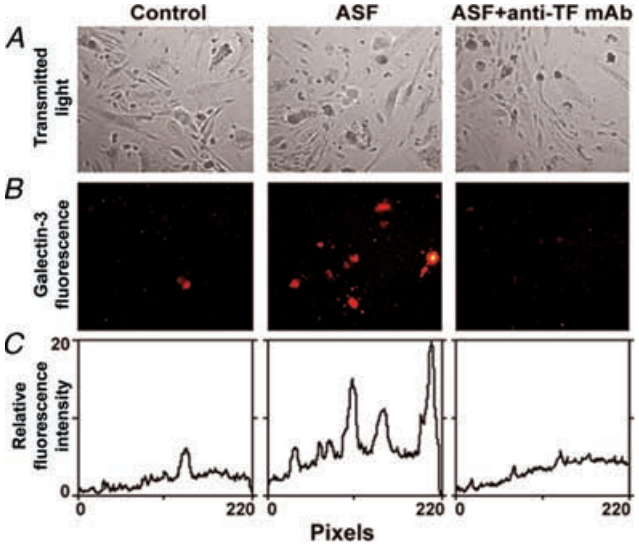

Figure 5. TF antigen-dependent galectin-3 cell surface mobilization on human bone marrow microvascular endothelium
Stimulation of human bone marrow microvascular endothelial cells with asialofetuin resulted in a rapid (25 min) increase in cell surface galectin-3 expression, which was almost completely abolished by anti-TF antigen monoclonal antibody. *A*, transmitted light images of the fields analysed for galectin-3-associated immunofluorescence in *B*. *C*, quantification of the galectin-3 cell surface expression using NIH imaging software.

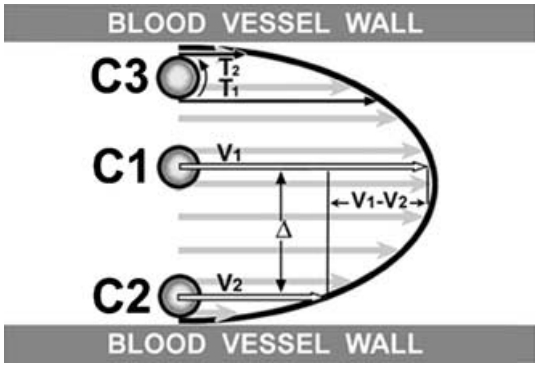

Figure 6. Parabolic profile of velocity distribution in blood vessels
A decrease in tumour cell velocity $V_1 - V_2$ reflects their displacement Δ from the centre of the stream toward the vascular wall, whereas both direct tumour–endothelial cell interactions and difference in torque $T_1 - T_2$ acting upon opposite tumour cell edges induce rolling response.

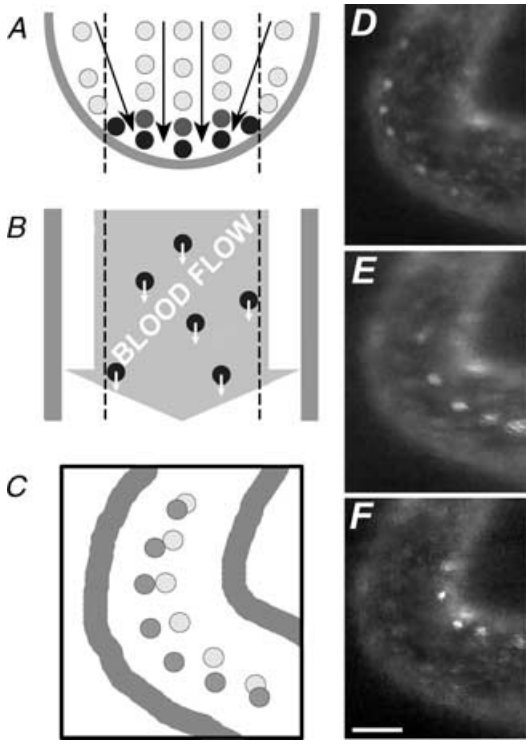

Figure 7. Cancer cell interactions with vascular walls determine their radial position and adhesive behaviour within perfused microvasculature
Sedimentation as a result of gravity would cause tumour cell displacement into the bottom part of a microvessel (*A*). Consequently, such cells would appear under a microscope as rolling along the centreline in a straight microvessel segment (*B*), or slightly deviating from the centreline as a result of out of centre forces in an arched microvessel (*D*). However, in reality, metastatic cells frequently interact with the lateral microvessel edges as in Fig. 1, or roll along both concave and convex vessel edges, as well as along the centreline, in arched microvessels. Scale bar in *D*–*F* (shown in *F*), 50 μm.

an increase in malignant cell adhesive interactions with vascular wall. However, the effects of gravity (if any) would remain the same throughout the course of the experiment, and cannot provide a feasible rationale for the observed gradual changes in tumour cell velocity and rolling. In addition, sedimentation as a result of gravity would cause neoplastic cell accumulation in the bottom portion of a vessel lumen (Fig. 7*A*). If that were the case, then we would observe interacting/rolling cells travelling mostly along the centreline of horizontally positioned blood vessels (Fig. 7*B* and *C*). However, in either straight or arched microvessel segments, we often observe cancer cells interacting with lateral 'edges' of the vessel wall (Figs 1 and 7*D* and *F*). These observations are consistent with the results on leucocyte adhesion previously reported by Firrell & Lipowsky (1989), showing that ∼50% of rolling leucocytes interact with lateral vessel 'edges' including the anterior and posterior vessel walls. It appears that under conditions of flow, hydrodynamic forces acting upon cancer cells largely compensate for the effects of gravity, and similarly to leucocyte rolling in venules (Ley & Gaehtgens, 1991), changes in endothelial properties, not in haemodynamics, are responsible for metastatic cell rolling in arterioles.

Nevertheless, haemodynamic factors (if present) could contribute potentially to the overall reduction in neoplastic cell velocities. In this study, we did not assess blood flow velocity independent of changes in tumour cell velocities. Therefore, we cannot completely rule out possible haemodynamic aberrations resulting from blood vessel reaction in response to cancer cell perfusion. However, when TF antigen-deficient non-metastatic MDA-MB-468 cells were perfused, they did not exhibit any decrease in velocity (Fig. 3*A*). Furthermore, blocking TF antigen with mAb abrogated changes in adhesion kinetics (Fig. 3*B*) and travelling velocities of highly metastatic MDA-MB-435 cells (Fig. 3*A*). These results indicate clearly that even if changes in haemodynamics took place, they were also TF antigen-dependent, i.e. resulting from microvascular reaction in response to TF antigen-mediated endothelial activation.

In summary, the results of this study demonstrate that microvascular endothelium in metastasis-prone tissues undergoes activation in response to desialylated cancer-associated carbohydrate structures (TF antigen) expressed on tumour cells and glycoproteins, manifested by cell surface mobilization of β-galactoside-binding lectin galectin-3. Such activation, preceding tumour cell arrest and retention in microcirculation, could play an important role in haematogenous breast and prostate cancer metastasis. The efficient inhibition of this process by anti-TF antigen antibody suggests that metastasis-associated endothelium activation could be an important target for developing new approaches to cancer therapy. Of note, the metastasis-associated endothelium activation described here occurs in response to carbohydrate stimuli in the absence of cytokines. To the best of our knowledge, this is the first report describing such carbohydrate-mediated endothelium activation. As desialylated cancer-associated carbohydrate structures such as TF antigen could appear under special circumstances on the surfaces of normal cells as well (e.g. aged erythrocytes), this phenomena could also be of general physiological significance.

References

Abbitt KB, Rainger GE & Nash GB (2000). Effects of fluorescent dyes on selectin and integrin-mediated stages of adhesion and migration of flowing leukocytes. *J Immunol Methods* **239**, 109–119.

Bresalier RS, Byrd JC, Wang L & Raz A (1996). Colon cancer mucin: a new ligand for the β-galactoside-binding protein galectin-3. *Cancer Res* **56**, 4354–4357.

Butcher EC (1991). Leukocyte-endothelial cell recognition: three (or more) steps to specificity and diversity. *Cell* **67**, 1033–1036.

Cooper CR, Bhatia JK, Muenchen HJ, McLean L, Hayasaka S, Taylor J, Poncza PJ & Pienta KJ (2002). The regulation of prostate cancer cell adhesion to human bone marrow endothelial cell monolayers by androgen dihydrosterone and cytokines. *Clin Exp Metastasis* **19**, 25–33.

Duffy MJ (1999). CA 15-3 and related mucins as circulating markers in breast cancer. *Ann Clin Biochem* **Pt 5**, 579–586.

Ellerhorst J, Nguyen T, Cooper DNW, Lotan D & Lotan R (1999). Differential expression of endogenous galectin-1 and galectin-3 in human prostate cancer cell lines and effects of overexpressing galectin-1 on cell phenotype. *Int J Oncol* **14**, 217–224.

Firrell JC & Lipowsky HH (1989). Leukocyte margination and deformation in mesenteric venules of rat. *Am J Physiol* **256** *Heart Circ Physiol* **25**, H1667–H1674.

Gaehtgens P, Ley K, Pries AR & Muller R (1985). Mutual interactions between leukocytes and microvascular blood flow. *Prog Appl Microcirc* **7**, 15–28.

Glinskii OV, Huxley VH, Turk JR, Deutscher SL, Quinn TP, Pienta KJ & Glinsky VV (2003*a*). Continuous real time ex vivo epifluorescent video microscopy for studying cancer cell interactions with dura mater microvasculature. *Clin Exp Metastasis* **20**, 451–458.

Glinsky VV, Glinsky GV, Glinskii OV, Huxley VH, Turk JR, Mossine VV, Deutscher SL, Pienta KJ & Quinn TP (2003*b*). Intravascular metastatic cancer cell homotypic aggregation at the sites of primary attachment to the endothelium. *Cancer Res* **63**, 3805–3811.

Glinsky VV, Glinsky GV, Rittenhouse-Olsen K, Huflejt ME, Glinskii OV, Deutscher SL & Quinn TP (2001). The role of Thomsen–Friedenreich antigen in adhesion of human breast and prostate cancer cells to the endothelium. *Cancer Res* **61**, 4851–4857.

Glinsky VV, Huflejt ME, Glinsky GV, Deutscher SL & Quinn TP (2000). Effects of Thomsen–Friedenreich antigen-specific peptide P-30 on β-galactoside-mediated homotypic aggregation and adhesion to the endothelium of MDA-MB-435 human breast carcinoma cells. *Cancer Res* **60**, 2584–2588.

Khaldoyanidi SK, Glinsky VV, Sikora L, Glinskii AB, Mossine VV, Quinn TP, Glinsky G.V & Sriramarao P (2003). MDA-MB-435 human breast carcinoma cell homo- and heterotypic adhesion under flow conditions is mediated in part by Thomsen–Friedenreich antigen–galectin-3 interactions. *J Biol Chem* **278**, 4127–4134.

Krause T & Turner GA (1999). Are selectins involved in cancer metastasis? *Clin Exp Metastasis* **17**, 183–192.

Lawrence MB & Springer TA (1991). Leukocytes roll on selectin at physiologic flow rates: distinction from and prerequisite for adhesion through integrins. *Cell* **65**, 859–873.

Lehr JE & Pienta KJ (1998). Prefential adhesion of prostate cancer cells to a human bone marrow endothelial cell line. *J Natl Cancer Inst* **90**, 118–123.

Ley K, Cerrito M & Arfors K-E (1991). Sulfated polysaccharides inhibit leukocyte rolling in rabbit mesentery venules. *Am J Physiol* **260**, H1667–H1673.

Ley K & Gaehtgens P (1991). Endothelial, not hemodynamic differences are responsible for preferential leukocyte rolling in rat mesenteric venules. *Circ Res* **69**, 1034–1041.

McEver RP (1997). Selectin–carbohydrate interactions during inflammation and metastasis. *Glycoconjugate J* **14**, 585–591.

Nangia-Makker P, Hogan V, Honjo Y, Baccarini S, Tait L, Bresalier R & Raz A (2002). Inhibition of human cancer cell growth and metastasis in nude mice by oral intake of modified citrus pectin. *J Natl Cancer Inst* **94**, 1854–1862.

Orr FW & Wang HH (2001). Tumor cell interactions with the microvasculature: a rate-limiting step in metastasis. *Surg Oncol Clinics North America* **10**, 357–381.

Padera TP, Stoll BR, So PTC & Jain RK (2002). Conventional and high-speed intravital multiphoton laser scanning microscopy of microvasculature, lymphatics, and leukocyte–endothelial interactions. *Mol Imaging* **1**, 9–15.

Rittenhouse-Diakun K, Xia Z, Pickhardt D, Morey S, Baek M-G & Roy R (1998). Development and characterization of monoclonal antibody to T-antigen (Galβ1–3galnac-α-O).*Hybridoma* **17**, 165–173.

Rood PML, Von Calafat J, dem Borne AEG, Kr Gerritsen WR & van der Schoot CE (2000). Immortalisation of human bone marrow endothelial cells: characterization of new cell lines. *Eur J Clin Invest* **30**, 618–629.

Rubin MA, Pitzi M, Mucci N, Smith DC, Wojno K, Korenchuk S & Pienta KJ (2000). Rapid ('warm') autopsy study for procurement of metastatic prostate cancer. *Clin Cancer Res* **6**, 1038–1045.

Ruoslahti E & Rajotte D (2000). An address system in the vasculature of normal tissues and tumors. *Annu Rev Immunol* **18**, 813–827.

Satoh M, Numahata K, Kawamura S, Saito S & Orikasa S (1998). Lack of selectin-dependent adhesion in prostate cancer cells expressing sialyl Le (x). *Int J Urol* **5**, 86–91.

Segre G & Silberberg A (1962). Behavior of microscopic rigid particles in Poiseuille flow II. Experimental results and interpretation. *J Fluid Mech* **14**, 136–157.

Acknowledgements

This work was supported in part by National Institutes of Health grants P20 CA86290 and P-50 CA103130-01 (V.V.G.); T32 HL07094 (O.V.G.); R37 HL-42528-13 and PO1 HL52490-06 (V.H.H.); RO1 HL-36088-16 (J.R.T.); and P50 CA69568 (K.J.P.).